

MODELLING AND DEVELOPMENT OF EXPONENTIAL HORN-ASSISTED FIBER-OPTIC SENSOR FOR PARTIAL DISCHARGE MONITORING IN HV SUBSTATIONS

Krishanlal Adhikari¹, Chiranjib Koley², and Nirmal Kumar Roy³

¹EE Department, NIT Durgapur, Durgapur-713209, West Bengal, Email:
krishanlaladhikari@gmail.com

²Professor, EE Department, NIT Durgapur, Durgapur-713209, West Bengal, Email:
chiranjib.koley@gmail.com

³Professor, EE Department, NIT Durgapur, Durgapur-713209, West Bengal, Email:
roy.nk2003@gmail.com

Abstract:

Partial discharge (PD) is considered as an important marker of insulation deterioration of high voltage (HV) apparatus. Therefore, PD monitoring is crucial for ensuring the sound and safe operation of high-voltage (HV) substations. In this work, an optical fiber-based, sensitive, and simple acoustic PD sensor module is proposed, which introduces a fiber-to-fiber coupling arrangement placed at the internal focal region of a suitably modelled exponential horn-shaped waveguide. The exponential horn concentrates the PD-generated ultrasonic pressure waves, thereby amplifying the acoustic emission and resulting in a larger impact at the focal point. These impacts cause small transverse misalignments between the transmitting and receiving optical fibers of the fiber-to-fiber coupling arrangement, which alter the coupling efficiency and result in measurable changes in the intensity of the coupled light. This intensity-modulation scheme eliminates the need for sophisticated optical components, such as fiber Bragg gratings or tunable lasers, resulting in a cost-effective and compact system suitable for installation in substations for monitoring PD events. The horn-assisted sensor offers a better signal-to-noise ratio and a broader detection bandwidth, which would otherwise be challenging. Furthermore, the performance of the proposed sensor is compared with the standard IEC 60270-based electrical detection system in the laboratory, which confirms the comparable detection capability of the proposed method. The system demonstrates reliable performance even in the presence of significant electromagnetic interference, making it suitable for identifying early-stage PD activity across air, oil, and solid insulation. The findings suggest that the introduced horn-guided fiber-optic sensor holds great potential for real-time partial discharge monitoring and evaluating the condition of high-voltage substation assets.

Keywords: Exponential horn-shaped waveguide, fiber-to-fiber coupling, high voltage assets, insulation deterioration, partial discharge.

1. Introduction

HV power apparatuses are valuable assets in a substation. Insulation failure is reported to be the most common reason behind the sudden failure of power equipment [1]. PD activity indicates the

early symptom of insulation degradation in power apparatus; hence, Partial discharge (PD) monitoring is critical for high-voltage substations. Localized discharge events initiate progressive deterioration within solid, liquid, or gaseous insulating media, which can ultimately lead to insulation breakdown if not detected in a timely manner. The elevated electrical, thermal, and environmental stresses on the HV apparatus assist the aging processes and diminish the lifespan of HV assets, such as transformers, bushings, cables, and GIS components. Online PD monitoring provides crucial insights for evaluating insulation health, identifying developing issues, and facilitating prompt maintenance decisions. As a result, monitoring PD activities plays a crucial role in predictive maintenance strategies to enhance reliability and operational security in high-voltage substations [2]. Partial discharge detection can be achieved through various conventional and nonconventional techniques that are fundamentally based on distinct physical phenomena [3]. The traditional electrical [4] approach detects the high-frequency current pulses produced during discharge. In chemical detection [5] by dissolved gas analysis, the presence of gases emitted from insulation breakdown is investigated to explore the nature and intensity of partial discharge. The ultrahigh-frequency (UHF) method [6] is based on capturing the electromagnetic radiation emitted during the PD phenomenon in the 300–3000 MHz range. The principle behind PD acoustic detection is to detect the ultrasonic waves emitted during PD events caused by the evaporation of the insulating medium [7]. In optical detection [8], the broadband light emitted during PD activities is sensed by a fluorescent optical fiber sensor.

The standard electrical method (IEC 60270) [4] is the most accurate way to measure the apparent charge associated with PD; however, it requires direct electrical contact and is highly sensitive to electromagnetic noise, making it challenging to use online in a substation. HFCT sensors [9] can pick up high-frequency PD current pulses through grounding paths. They are very sensitive, but they require direct electrical access and are highly susceptible to electromagnetic noise in substations. TEV sensors [10] respond to temporary earth voltages on metal surfaces and are easy to install. However, their performance is affected by the condition of the surface, the quality of the grounding, and outside interference, which makes them less reliable in harsh substation environments. Chemical detection [5], particularly dissolved gas analysis, is effective in identifying long-term insulation damage in oil-filled equipment. However, it cannot be implemented for online monitoring purposes, and isn't suitable for air-insulated or gas-insulated systems. UHF detection [6] captures the electromagnetic radiation associated with PD events in the higher frequency spectrum, i.e., the MHz to GHz range, and is highly promising in terms of sensitivity and response time. However, it requires wideband sensors designed to cover higher frequencies, which poses design complexity, and doesn't work well in a substation environment due to high attenuation, multipath reflections, and associated interference from different sources. Acoustic emission techniques [7] [11] detect the ultrasonic waves emitted during PD and monitor them without electromagnetic interference; however, the generated acoustic signals are heavily attenuated and reflected by structural paths and often suppressed by mechanical noise. Hence, noninvasive piezoelectric sensors [12] suffer from a low signal-to-noise ratio. Optical methods

based on light emission measurements are completely immune to EMI and can even work without any active sensors. However, they often require high-end, expensive hardware equipment and require an optical path from source to sensor.

In recent times, the optical fiber-based acoustic sensor has gained considerable popularity, as these sensors offer highly sensitive ultrasonic detection capabilities with minimal transmission loss, maintaining immunity to electromagnetic interference, inherent electrically passive dielectric nature, and compactness, which establishes them as a superior alternative for invasive applications near HV assets [13]. Fiber Bragg grating (FBG) sensors detect strain-induced wavelength shifts with good sensitivity and directional response. [14] experimentally established that FBG-based systems can reliably detect PD activity and serve as effective alternatives to conventional electrical measurement systems. Still, such measurements involve costly, tunable lasers or optical spectrum analyzers and are highly sensitive to temperature variations. Interferometric sensors, such as Mach–Zehnder [15], Fabry–Perot [16], Sagnac [17], and Michelson [18] configurations, offer exceptionally high acoustic sensitivity by measuring phase changes in the optical path. They still require coherent light sources, long sensing arm, and precise arm balancing, which makes them susceptible to ambient vibrations and changes in temperature. Side-polished [19] and etched fiber [20] sensors enhance acoustic coupling by reducing the cladding thickness. However, this reduces the mechanical strength and increases the likelihood of physical damage during installation.

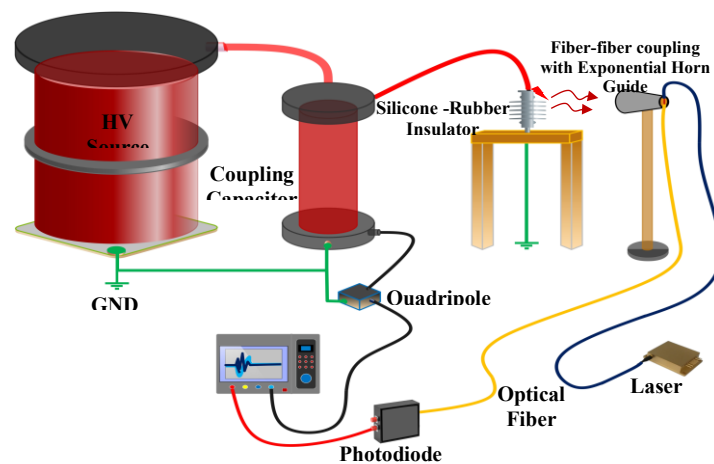


Fig. 1. Schematic representation of the exponential horn guided intensity modulated optical fiber-based PD monitoring scheme, along with the conventional IEC 60270 electrical detection system.

Phase-shifted FBG is more sensitive and can detect narrowband signals. [21] proposes a PS–FBG–based ultrasonic sensing system for highly sensitive, EMI-immune early detection of partial discharge in power transformers. With optimized wavelength scanning and a strong ultrasonic response, the PS-FBG sensor demonstrated 17.5 times higher sensitivity than PZT in transformer-oil tests. However, it requires advanced manufacturing methods and careful thermal compensation.

These optical sensing methods exhibit good performance, but their real-life application is often impractical due to complexity, high manufacturing costs, sensitivity to environmental factors, and the need for stable optical interrogation systems. Hence, there exists no prominent solution that can achieve all the benefits associated with optical fiber-based sensors, while manifesting a compact, cost-effective architecture, and yet achieving enhanced sensitivity in the desired bandwidth.

In our previous study [22], we proposed a microstructure-based sensor consisting of a fiber-to-fiber coupling arrangement and experimentally verified its potential in real-life invasive applications, particularly within a transformer. In this study, we propose an exponential horn-assisted fiber-optic sensor based on a fiber-to-fiber coupling arrangement and experimentally verify its performance for PD monitoring in substations. The main contributions of the paper are as follows;

- Design and development of an exponential horn guide for the intensity modulated sensor through mathematical modelling and optimization that enhances the directional sensitivity, thereby improving inspection accuracy compared to conventional designs.
- The development of a lightweight, handheld system suitable for PD monitoring in substation.
- Detection of various types of PD events, i.e., corona, internal discharge, and surface discharge, using the developed system, and comparing its performance with that of the standard IEC 60270-based system to investigate the potential of the proposed system.

The remainder of the paper is organized as follows. Section II discusses the architecture of the proposed sensing system. Section III presents the experimental setup and methodology to investigate the performance of the developed system. Section IV presents the results of the experimental study, followed by discussion. Finally, Section V summarizes the main findings and explores the scope for future work.

2. Mathematical Modelling and Development of the Sensor Module

The sensor module comprises two sections, i.e, the fiber-to-fiber coupling arrangement and the exponential horn waveguide. These two sections are designed separately and then assembled together to construct the sensor module.

A. Design of the Fiber-to-Fiber Coupling Arrangement

The fiber-to-fiber coupling arrangement consists of a straightforward configuration, where a transmission fiber is kept in near proximity to the receiving fiber, allowing light to couple between the two fibers through the free space between them. The transmitting fiber is rigidly attached in place in the focal region of the exponential horn, while the receiving fiber is mounted to a small and flexible structure. The immobilized fiber carries light from the source, and the flexible fiber gathers the light that has been emitted. The motion induced in the flexible fiber by concentrated PD-generated acoustic waves alters the coupling efficiency of the configuration; hence, the intensity received by the receiving fiber becomes a function of the PD-emitted acoustic wave. The

fixed-flexible arrangement of the two fibers is placed at the focal point of an exponential horn to experience the maximum thrust from the PD-generated acoustic waves. This is the location where the incoming acoustic pressure is concentrated most. The rigid fiber is bonded to a stable base plate, which keeps the fiber in the same position, even in the presence of external movements. In contrast, the receiving fiber is attached to a small, flexible part that only bends when sound waves are present in the focal zone of the horn. A small deflection of the flexible structure causes a significant change in the optical coupling (O_c), making the system highly sensitive towards the PD-generated ultrasonic waves as shown in (1).

$$\left\{ \begin{array}{l} O_c = -10 \log \frac{16 r_f^2 r_m^2}{(n_f + n_m)^4} \exp \frac{-Q^2 s_p^2 F^2}{2} \\ \text{where } Q = \frac{2\pi r_m}{\lambda} \ \& \ F = \frac{of_l}{Q s_p^2} \end{array} \right. \quad (1)$$

where the refractive index of the fiber and the medium are r_f and r_m , respectively. The wavelength of the source is λ ; the lateral offset is of_l and s_p is the spot size of the fiber.

To explore the feasibility of the flexible structure vibrating in sync with the incoming acoustic waves, the dynamic response of the structure is investigated. To assess the viscous damping response of the structure, the structure is mathematically modeled as a second-order spring (k) – mass (M) – damper (B) system, and its frequency of natural oscillations, as well as the deformation, is expressed in the form of model variables presented in (2).

$$\left\{ \begin{array}{l} f_n = \frac{1}{2\pi} \sqrt{\frac{k}{M} - \left(\frac{B}{2M}\right)^2} \\ \delta = \frac{\Delta F l^4}{16 Y T^3} \end{array} \right. \quad (2)$$

Where, ΔF is the peak differential pressure exerted on the structure, l and T are the length and thickness of the structure, Y represents the Young’s modulus of the structural material.

It is profoundly observed that with respect to the fundamental structure parameters, i.e., l , T , Y , the natural frequency of oscillations and the deformation are inversely related; hence, to achieve the desired sensitivity with a broad bandwidth, a multiobjective fitness function is formulated as shown in (3) and optimized using the non-dominated sorting genetic algorithm.

$$\{\max: F(l, T, Y) = f_n(l, T, Y) + \delta(l, T, Y)\} \quad (3)$$

Based on the optimization outcomes, the flexible structure is designed and placed in close proximity to the fixed structure at the focal region of the waveguide. Thereafter, the optical fibers are precisely mounted and aligned on the fixed and flexible structure to form the fiber-to-fiber coupling arrangement.

B. Mathematical Modelling and Optimization of the Exponential Horn Waveguide

Sound waves lose some of their power before they reach the sensor and scatter in all directions in the absence of a waveguide. This is particularly valid for ultrasonic elements with high frequencies. These waves are guided along a specific path by a well-designed waveguide, which maximizes signal concentration at the detection location and reduces signal loss. By filtering out particular frequencies, it lowers undesired noise and raises the signal-to-noise ratio overall. Due to the involvement of waveguide the sensor may be positioned away from high-voltage locations and yet record sound energy. The exponential horn waveguide is used in this investigation because its profile gradually widens, reducing impedance variations and acoustic reflections, enhancing the efficiency of energy delivery to the sensor. Due to the shape's inherent ability to concentrate pressure at the throat, weak ultrasonic signals by PD activity become more prominent. The narrowing effect increases the sensitivity of the sensor without the use of electronics, hence it works as a passive sound amplifier. Additionally, the horn enhances directionality, which reduces the interference of outside noise. Minimizing the distortion of the sound waveform, the proposed waveguide preserves the purity of the signal.

The profile of the exponential horn is defined by the relation as presented in (4)

$$\begin{cases} R(x) = R_t e^{mx} \\ \text{Where} \\ m = \left(\frac{1}{L} \cdot \ln \frac{R_m}{R_t}\right) \end{cases} \quad (4)$$

Where, $R(x)$ represents the consequive radius at a distance x from the throat of the waveguide. R_t and R_m are the throat and mouth radius, respectively, and L presents the length of the horn. Hence, the gain offered by the horn can be written as (5).

$$\text{Gain} = 20 \cdot \log \frac{R_m}{R_t} \quad (5)$$

The exponential horn accumulates a broader frequency range, hence widening the effective bandwidth of the sensor. The relation between the cutoff frequency and exponential costant is presented in (6), where C presents the speed of sound in the air medium.

$$F_c = \frac{C}{2 \cdot \pi \cdot m} \quad (6)$$

Hence, the choice of cutoff frequency is crucial for highly sensitive detection of Pd acoustic emissions. To keep a balance between the gain and bandwidth of the proposed exponential horn profile, an optimization framework has been formulated based on R_m , R_t , and L as variables. The formulated fitness function is presented in (7).

$$\begin{cases} F(x) = \alpha \left(20 \cdot \log \frac{R_m}{R_t} \right) + \beta \left[\left(1 + \frac{F_c}{50000} \right) \int_{20000}^{80000} e^{-\frac{(F-50000)^2}{2.15000^2}} dF \right] + Pn \\ x = [R_m, R_t, L] \\ F_c = \frac{c}{2\pi} \cdot \frac{1}{L} \cdot \ln \frac{R_m}{R_t} \end{cases} \quad (7)$$

Here, x is the design variable vector, α and β are the weighting factors associated with gain and sensitivity, respectively. The Pn determines design constraints, ensuring R_m and R_m ratio less than 25. Thus, optimizing this aforementioned fitness function using the gradient descent and genetic algorithm method, a suitable design of the horn is finalized, which offers a significant gain in the desired frequency bandwidth of PD emission. Thus, the exponential horn waveguide is manufactured, and the fiber-to-fiber coupling arrangement is installed in it to develop the sensor module.

3. Experimental Setup

Following the development of the exponential horn-assisted fiber-to-fiber coupling-based intensity-modulated optical fiber sensor, its performance is experimentally verified in the laboratory. Primarily, partial discharge testing has been carried out on three different samples representing corona, internal, and surface discharges. To emulate corona discharge in a laboratory, a sharp metal electrode kept in air is excited by high voltage. An 11 KV silicone rubber insulator is excited by high voltage in wet conditions to generate surface discharge phenomena. A Nomex paper is placed between the needle flat electrode arrangement, which is excited by high voltage, to facilitate internal discharge. The developed sensor and the standard IEC 60270-based electrical detection method simultaneously measured all three discharge events.

In the conventional electrical detection method, the test objects are excited using a 300 kV, 0.5 ampere high-voltage test transformer and a 300 kV, 100 pF capacitive voltage divider. The test object is kept in parallel with the coupling capacitor. The coupling capacitor is connected to a quadrupole, followed by a data acquisition unit. In this condition, the voltage across the test object is gradually increased until PD phenomena are initiated.

During PD monitoring using the proposed method, the developed sensor module his placed close to the discharge source as shown in Fig. 2. The fiber-to-fiber coupling arrangement, located inside the sensor module, is excited by a laser source. The incoming laser, transmitted through the transmitting fiber, is coupled to the receiving optical fiber placed on the flexible structure through air. The coupled laser light from the receiving fibre is guided to a photodetector and a transimpedance amplifier unit, where the received light is converted to an equivalent voltage. Thereafter, the photo detector output is connected to the oscilloscope.

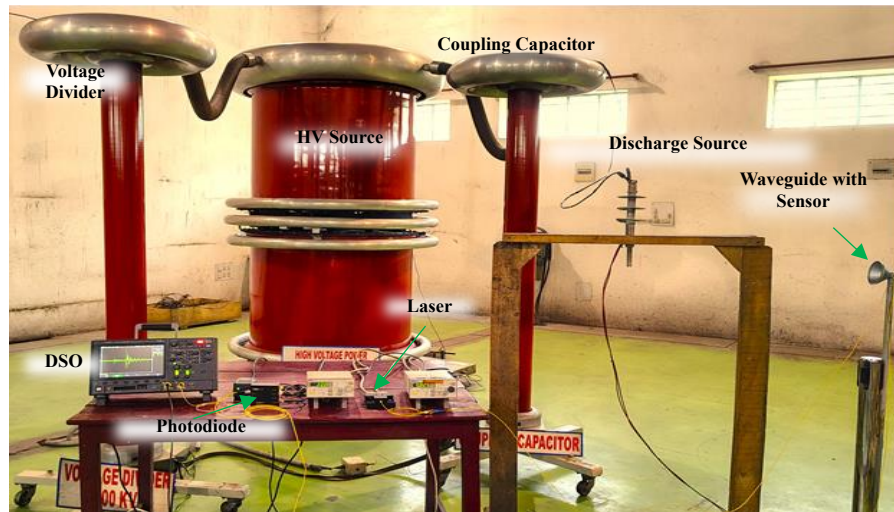


Fig. 2. Real-time monitoring of PD using the proposed method and the standard electrical detection method simultaneously.

Before starting the experiment, the standard electrical detection system was calibrated using a standard PD calibrator. After calibration, the inherent noise associated with the high-voltage setup was found to be 7 pc. For the developed sensor under unexcited conditions, it was observed that the coupling efficiency of the fiber-to-fiber arrangement was around 73%. For simultaneous data acquisition, the test samples were excited using high voltage until PD inception occurred inside the test samples. After that, the response from both the standard and proposed methods was captured and digitized using an oscilloscope simultaneously. To extract the frequency content related to the proposed sensor, single PD pulses are extracted from the received signals and further processed using the discrete Fourier transform in MATLAB software. To obtain the phase-resolved partial discharge (PRPD) pattern from both detection systems, PD events were monitored for a span of 15 minutes, along with the supply voltage signal. Thereafter, PD events for individual supply cycles are segregated and overlapped phasewise to form the PRPD pattern.

4. Results and Discussion

It is evident from Fig. 3 that both the detection methods confirm the discharge phenomenon. From the time domain signals as detected by both methods, it is evident that the high-frequency impulsive pulses appear during the rising part of the supply voltage, which is consistent with the physics behind corona discharge. This shows that both systems can detect the same discharge events even though they work on different physical principles. The discharge magnitudes cluster together in specific phase intervals, primarily between 0° and 90° , according to the phase-resolved PD (PRPD) patterns derived from the two approaches. Ionization occurs when the local electric field surpasses the inception threshold, which is consistent with the usual corona behavior. Due to its increased sensitivity to charge transfer, the electrical approach produces a more concentrated dispersion of PD points. In contrast, the acoustic sensor has strong mechanical fingerprints for more.

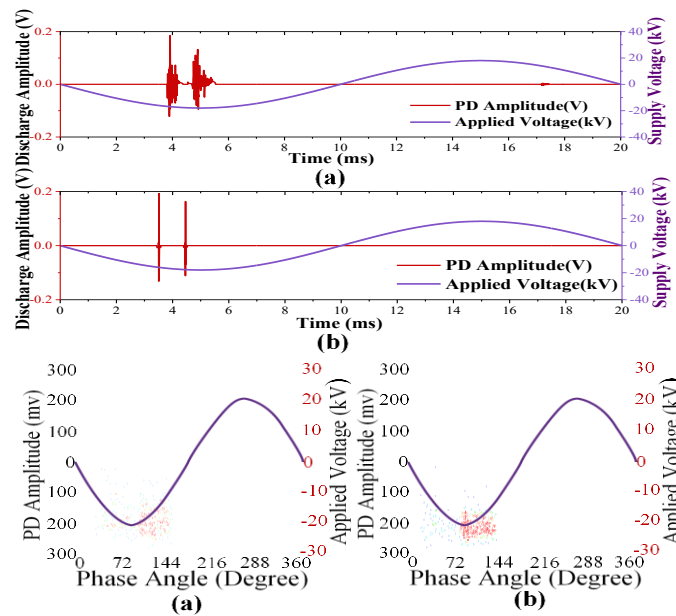


Fig. 3. PD pulses and corresponding PRPD patterns as recorded by the (a) proposed and (b) standard electrical detection method during monitoring corona discharge phenomenon.

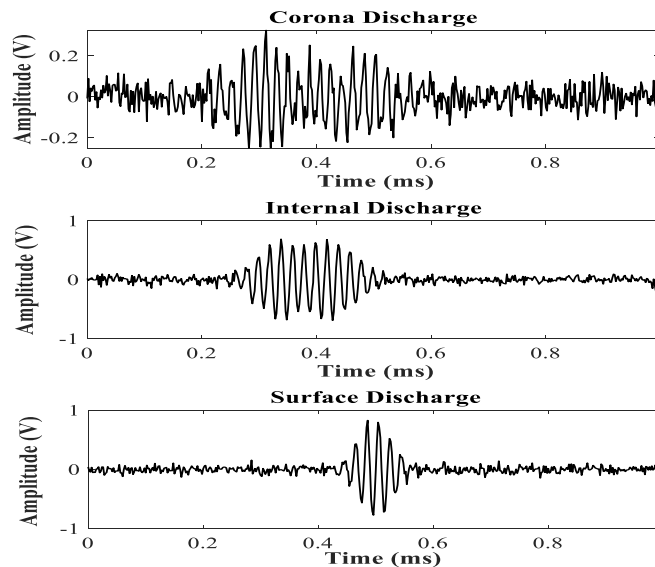


Fig. 4. Nature of PD pulses detected by the proposed method during corona, internal, and surface discharge powerful events without any EMI.

It is observed from Fig. 4 that the proposed method can distinctly detect different PD phenomena, i.e., corona, internal discharge, and surface discharge. The pulses detected during corona discharge have considerably low amplitude and SNR, while the spread of the detected pulse is wide, having a multiple-frequency superimposed nature that is consistent with distributed ionization and repeated streamer pulses; this makes corona events detectable but of relatively low

mechanical/acoustic strength. The internal discharge shows a much larger, well-formed oscillatory packet with a pronounced, longer-duration carrier burst, indicating a stronger, higher-

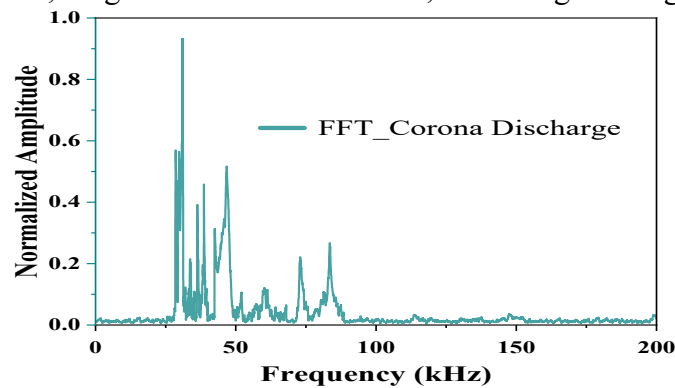


Fig. 5. Frequency distribution of the detected PD pulse as recorded by the proposed method during corona discharge energy event originating within a cavity or void; such events produce both strong electrical pulses and clear acoustic shock signatures, aiding confident identification. Surface discharge is characterized by a short, sharp oscillatory burst of intermediate duration but similar peak amplitude to internal PD; its narrower envelope and quicker decay reflect localized surface streamer activity and produce a distinctive temporal profile useful for discrimination. Hence, it can be concluded that the proposed sensor has the capacity to distinctly detect various PD sources commonly encountered in HV substations.

Fig. 5 illustrates the frequency bandwidth of the proposed sensor, confirming its broadband nature as depicted by the distributed peaks along the frequency obtained from the fast Fourier transform (FFT) of the recorded PD pulses.

5. Conclusions

The result and associated discussions in Section 5 establish that the horn assistant optical fibre-based sensor can accurately detect different PD phenomena, such as corona, internal discharge, and surface discharge, with a similar level of efficiency to the standard electrical detection method. It is also observed that the proposed method effectively distinguishes between different types of discharges commonly observed in HV substations with a broadband detection sensitivity. Therefore, it can be concluded that the proposed sensor can serve as a suitable and progressive PD monitoring solution for HV substations, offering additional advantages of being cost-effective and interference-free. The future scope of the present study includes investigating more advanced structures as a waveguide to enhance detection sensitivity and exploring better packaging for the entire sensor module, which aids reliability.

References

- [1] M. Pompili, "Partial discharge development and detection in dielectric liquids," in *IEEE Transactions on Dielectrics and Electrical Insulation*, vol. 16, no. 6, pp. 1648-1654, December 2009, doi: 10.1109/TDEI.2009.5361585.

- [2] L. Calcara, M. Pompili and F. Muzi, "Standard evolution of Partial Discharge detection in dielectric liquids," in *IEEE Transactions on Dielectrics and Electrical Insulation*, vol. 24, no. 1, pp. 2-6, Feb. 2017, doi: 10.1109/TDEI.2016.006499.
- [3] W. Zhang, P. Lu, W. Ni, W. Xiong, D. Liu and J. Zhang, "Gold-Diaphragm Based Fabry-Perot Ultrasonic Sensor for Partial Discharge Detection and Localization," in *IEEE Photonics Journal*, vol. 12, no. 3, pp. 1-12, June 2020, Art no. 6801612, doi: 10.1109/JPHOT.2020.2982460.
- [4] *Partial Discharge Measurements*, Standard IEC 60270, 2015.
- [5] W. Inwanna, S. Waiwicha, P. Vanijkirati, S. Monkolsatitpong, K. Chumpiboon and N. Pattanadech, "Partial Discharge and Dissolved Gas Analysis on 22kV MV Oil-type Transformer – Case Study," *2024 IEEE 14th International Conference on the Properties and Applications of Dielectric Materials (ICPADM)*, Phuket, Thailand, 2024, pp. 150-153, doi: 10.1109/ICPADM61663.2024.10750560.
- [6] X. Kong, C. Zhang, C. Hou, X. Lin and B. Du, "UHF Sensor for Partial Discharge Detection Based on Coplanar Waveguide Feeding," in *IEEE Sensors Journal*, vol. 24, no. 17, pp. 28119-28128, 1 Sept.1, 2024, doi: 10.1109/JSEN.2024.3427412.
- [7] S. Kanakambaran, R. Sarathi and B. Srinivasan, "Robust Classification of Partial Discharges in Transformer Insulation Based on Acoustic Emissions Detected Using Fiber Bragg Gratings," in *IEEE Sensors Journal*, vol. 18, no. 24, pp. 10018-10027, 15 Dec.15, 2018, doi: 10.1109/JSEN.2018.2872826.
- [8] Jun Jiang; Guoming Ma, "Partial Discharge Detection with Optical Methods," in *Optical Sensing in Power Transformers*, IEEE, 2021, pp.137-188, doi: 10.1002/9781119765325.ch5.\
- [9] X. Gu, Y. Xu, R. Xia, S. Meng and Y. Wang, "On-line calibration of partial discharge monitoring for power cable by HFCT method," *2016 IEEE Electrical Insulation Conference (EIC)*, Montreal, QC, Canada, 2016, pp. 40-44, doi: 10.1109/EIC.2016.7548561.
- [10] F. Guastavino, L. D. Giovanna, F. Gallesi and E. Torello, "Transient Earth Voltage Sensor Measurements as a Nonintrusive Tool for Partial Discharge Analysis in Switchgears," in *IEEE Transactions on Dielectrics and Electrical Insulation*, vol. 31, no. 6, pp. 2930-2937, Dec. 2024, doi: 10.1109/TDEI.2024.3470755.
- [11] R. Ghosh, B. Chatterjee and S. Dalai, "A method for the localization of partial discharge sources using partial discharge pulse information from acoustic emissions," in *IEEE Transactions on Dielectrics and Electrical Insulation*, vol. 24, no. 1, pp. 237-245, Feb. 2017, doi: 10.1109/TDEI.2016.006080.
- [12] S. N. Meitei, "Partial Discharge Detection Using Piezoelectric Sensors on Power Transformer: A Review," in *IEEE Sensors Journal*, vol. 24, no. 9, pp. 13730-13742, 1 May1, 2024, doi: 10.1109/JSEN.2024.3379037.

- [13] Z. Meng, C. He, J. Liu and J. Geng, "Detection and Propagation Characteristics of Partial Discharge Optical Signal Based on Fluorescent Fiber Sensor," in *IEEE Sensors Journal*, vol. 24, no. 19, pp. 30004-30013, 1 Oct.1, 2024, doi: 10.1109/JSEN.2024.3421514.
- [14] B. Sarkar, C. Koley, N.K. Roy, P. Kumbhakar, "Condition monitoring of high voltage transformers using Fiber Bragg Grating Sensor," in *Measurement*, vol. 74, pp. 255-267, 2015, ISSN 0263-2241, <https://doi.org/10.1016/j.measurement.2015.07.014>.
- [15] P. Zhang, Y. Hao, Z. Shen, B. Yan and L. Li, "Acoustic-Enhanced Fiber-Optic MZI Sensing Technology for Partial Discharge Detection in Silicone Rubber Insulation," in *IEEE Sensors Journal*, vol. 25, no. 20, pp. 37989-37999, 15 Oct.15, 2025, doi: 10.1109/JSEN.2025.3607868.
- [16] W. -c. ZHANG, Q. -c. CHEN, L. -y. ZHANG and H. ZHAO, "Fiber Optic Fabry-Perot Sensor with Stabilization Technology for Acoustic Emission Detection of Partial Discharge," *2018 IEEE International Conference on High Voltage Engineering and Application (ICHVE)*, Athens, Greece, 2018, pp. 1-4, doi: 10.1109/ICHVE.2018.8641995.
- [17] Y. Song *et al.*, "Partial Discharge Detection Based on Optimization of Optical Probe and Sagnac Interference," in *IEEE Transactions on Instrumentation and Measurement*, vol. 71, pp. 1-9, 2022, Art no. 9006509, doi: 10.1109/TIM.2022.3219483.
- [18] Y. Song, W. Chen, Z. Zhang, F. Liu, K. Wu and H. Tian, "Built-in Detection of Partial Discharge Ultrasound Signals in Gas Insulated Switchgear Using Michelson Fiber Optic Interferometer Sensor," *2022 IEEE International Conference on High Voltage Engineering and Applications (ICHVE)*, Chongqing, China, 2022, pp. 1-5, doi: 10.1109/ICHVE53725.2022.9961829.
- [19] Cheng Li, Xiaobin Peng, Hui Zhang, Chao Wang, Shangchun Fan, Shaoqing Cao, "A sensitivity-enhanced flexible acoustic sensor using side polished fiber Bragg grating," *Measurement*, vol. 117, pp. 252-257, 2018, ISSN 0263-2241, <https://doi.org/10.1016/j.measurement.2017.12.027>.
- [20] J. Jiang, H. -T. Song, G. -M. Ma, C. R. Li, Y. -T. Luo and H. -B. Wang, "Dissolved hydrogen detection in power transformer based on etched fiber Bragg grating," *2015 IEEE International Instrumentation and Measurement Technology Conference (I2MTC) Proceedings*, Pisa, Italy, 2015, pp. 422-427, doi: 10.1109/I2MTC.2015.7151305.
- [21] Tian, Tian, Xiu Zhou, Sihan Wang, Yan Luo, Xiuguang Li, Ninghui He, Yunlong Ma, Weifeng Liu, Rongbin Shi, and Guoming Ma. 2022. "A π -Phase-Shifted Fiber Bragg Grating Partial Discharge Sensor toward Power Transformers" *Energies* 15, no. 16: 5849.
- [22] K. Adhikari, C. Koley and N. Kumar Roy, "Development of Intensity Modulated Optical Fiber Based Partial Discharge Sensor for High Voltage Power Apparatus," in *IEEE Transactions on Dielectrics and Electrical Insulation*, vol. 31, no. 6, pp. 2905-2914, Dec. 2024, doi: 10.1109/TDEI.2024.3449793.